PERGAMON

International Journal of Heat and Mass Transfer 45 (2002) 2655–2665

International Journal of HEAT and MASS TRANSFER

www.elsevier.com/locate/ijhmt

# Forced convective boiling of ternary mixtures at high qualities

J.R. Barbosa Jr. [a,b], T. Kandlbinder [a,c], G.F. Hewitt [a,*]

[a] *Department of Chemical Engineering and Chemical Technology, Imperial College of Science, Technology and Medicine, London SW7 2BY, UK*

[b] *Departamento de Engenharia Mecânica, Universidade Federal de Santa, Catarina (UFSC), Florianópolis, SC 88040-900, Brazil*

[c] *MAN Roland Druckmaschinen AG, Stadtbachstrasse 1, 86135 Augsburg, Germany*

Received 24 April 2001; received in revised form 27 November 2001

**Abstract**

This paper deals with convective boiling of ternary mixtures in vertical tubes. Experiments were carried out in 8.58 m long, 25.4 mm ID, electrically heated test section using an *n*-pentane/*n*-hexane/iso-octane mixture (0.31/0.22/0.47 overall mole fraction). Bulk and wall temperatures as well as local heat transfer coefficients were measured. The results were compared with those obtained using an extension to ternary (and multicomponent) mixtures of the methodology proposed by J.R. Barbosa and G.F. Hewitt [Int. J. Heat Mass Transfer 44 (2001) 1465, 1475] for prediction of forced convective boiling of binary mixtures in upward annular flow. Interphase transfer of heat and mass is dealt with using two formulations: (i) a film method in which the diffusive fluxes are calculated via a linearly generalised Fick's Law [H.L. Toor, AIChE J. 10 (4) (1964) 460; W.E. Stewart, R. Prober, Ind. Eng. Chem. Fundam. 3 (3) (1964) 224], and (ii) an effective diffusivity method. Droplet entrainment and deposition are modelled via an interchange model that takes into account the local concentration non-equilibrium between the liquid film and the entrained droplets. As for the binary case, it is claimed that the deterioration in the heat transfer coefficient is due to a combined effect of droplet interchange and mass transfer resistance in the vapour side. © 2002 Published by Elsevier Science Ltd.

## 1. Introduction

Processes involving boiling of mixtures of two or more substances are widely encountered in industry. However, despite the technological relevance, there is a dearth of adequately predictive and design methods for forced convective boiling of multicomponent mixtures [5]. The majority of methods available in the literature for phase change heat transfer of mixtures deal with the binary case. Moreover, of the number of studies devoted to the multicomponent case, most are related to condensation [6,7]. A fairly refined methodology, and yet applicable to condenser design, is that based on film (or Colburn) methods. Taylor and Krishna [8] gave a comprehensive review of the generalisations of Fick's Law for multicomponent systems and their application to a Colburn method calculation framework. Basically, two approaches are used: (i) the Effective Diffusivity Method, where each constituent is assumed to transfer at a rate equal to that at which it would transfer if it alone were present in an arbitrarily chosen reference species at the same concentration, and (ii) the so-called Interactive Method, a more refined theory put forward by Toor [3] and Stewart and Prober [4], that assumes a linear dependence of the diffusive fluxes on *all* concentration driving forces. A description of calculation procedures for condenser design using both approaches is also presented by Webb [9].

A model for boiling of ternary refrigerant mixtures in horizontal pipes was proposed by Zhang et al. [10]. In the forced convective dominant region, use was made of a film methodology in which an effective diffusivity approach was employed to calculate the interfacial mass fluxes. Zhang et al. concluded that no essential difference was found between the mechanisms of boiling heat

* Corresponding author. Tel.: +44-20-759-45562; fax: +44-20-759-45564.

*E-mail address:* g.hewitt@ic.ac.uk (G.F. Hewitt).

0017-9310/02/$ - see front matter © 2002 Published by Elsevier Science Ltd.
PII: S0017-9310(01)00361-1

**Nomenclature**

*Roman*

| | |
|---|---|
| $[B_G]$ | matrix of mass transfer coefficients (m $s^{-1}$) |
| $c_p$ | specific heat capacity at constant pressure (J $kg^{-1}$ $K^{-1}$) |
| $d_T$ | diameter of tube (m) |
| $D$ | deposition rate (kg $m^{-2}$ $s^{-1}$) |
| $E$ | entrainment rate (kg $m^{-2}$ $s^{-1}$) |
| $[I]$ | unit matrix (dimensionless) |
| $I_p$ | diffusion interaction coefficient (dimensionless) |
| $L_A$ | length of pipe in annular flow (m) |
| $\dot{m}$ | mass flux (kg $m^{-2}$ $s^{-1}$) |
| $p$ | pressure (Pa) |
| $Pr$ | Prandtl number (dimensionless) |
| $\dot{q}$ | heat flux (W $m^{-2}$) |
| $Re$ | Reynolds number (dimensionless) |
| $s$ | thickness of layer (film method) (m) |
| $[S_c]$ | Schmidt number matrix (dimensionless) |
| $T$ | temperature (K) |
| $x$ | composition of liquid (mass fraction) |
| $y$ | composition of vapour (mass fraction) (dimensionless) |
| Y | auxiliary radial co-ordinate (m) (dimensionless) |
| $z$ | axial co-ordinate (m) |

*Greek symbols*

| | |
|---|---|
| $\alpha$ | heat transfer coefficent (W $m^{-2}$ $K^{-1}$) |
| $\delta$ | Maxwell–Stefan diffusion coefficients ($m^2$ $s^{-1}$) |
| $[\Delta]$ | matrix of mass diffusivity coefficients ($m^2$ $s^{-1}$) |
| $\Delta h_v$ | latent heat of vaporisation (J $kg^{-1}$) |
| $\lambda$ | thermal conductivity (W $m^{-1}$ $K^{-1}$) |
| $\eta$ | viscosity (N s $m^{-2}$) |
| $[\Phi]$ | finite flux correction matrix for mass transfer (dimensionless) |
| $\phi_T$ | finite flux correction factor for heat transfer (dimensionless) |
| $\rho$ | density (kg $m^{-3}$) |

*Subscripts*

| | |
|---|---|
| av | average |
| b | bulk |
| C | core |
| E | equilibrium |
| GC | vapour/gas core |
| $i$ | component identifier, $1 = n$-pentane, $2 = n$-hexane |
| I | interface |
| L | liquid phase |
| LE | entrained liquid |
| LF | liquid film |
| w | wall |

*Superscript*

| | |
|---|---|
| . | finite flux |

transfer in binary and ternary systems. As far as the present authors are aware, the interactive model has not previously been tested for multicomponent boiling.

This paper presents experimental and modelling studies on forced convective boiling of ternary mixtures at high qualities. Experiments were carried out using an *n*-pentane/*n*-hexane/iso-octane mixture undergoing phase change in a vertical, 25.4 mm ID, electrically heated test section. The proposed model is an extension of that for phase change of binary mixtures in annular flow [1,2]. The model takes into account phenomenological aspects of the flow regime (such as droplet entrainment and deposition) and uses a Colburn method to describe the interphase transfer of mass and heat. Both Interactive and Effective Diffusivity formulations for calculating the diffusive fluxes are implemented and compared. For the substances analysed, the results show that diffusive interaction effects are not significant. However, differences in composition between the entrained droplets and the liquid film seem likely to exert a significant influence.

In what follows, Section 2 describes the experimental work and procedure. In Section 3, the model and the main associated assumptions are reviewed. Section 4 presents the comparisons between modelling and experimental results. Finally, conclusions are drawn in Section 5.

## 2. Experimental work

### 2.1. Experimental facility

The experimental data were acquired using a high pressure multicomponent boiling facility situated at the AEA Technology plc site at Harwell, Oxfordshire, UK. The facility was operated under a collaborative experiment with the Heat Transfer and Fluid Flow Service (HTFS), the latter being part of AEA Technology. A schematic of the HTFS High Pressure Boiling facility is shown in Fig. 1(a). The rig consists of three loops, namely the circulating, pressurising and degassing loops. The main circuit contains the vertically oriented test section, a shell and tube condenser, a circulating pump, a 75 kW electrical pre-heater, a density meter (model

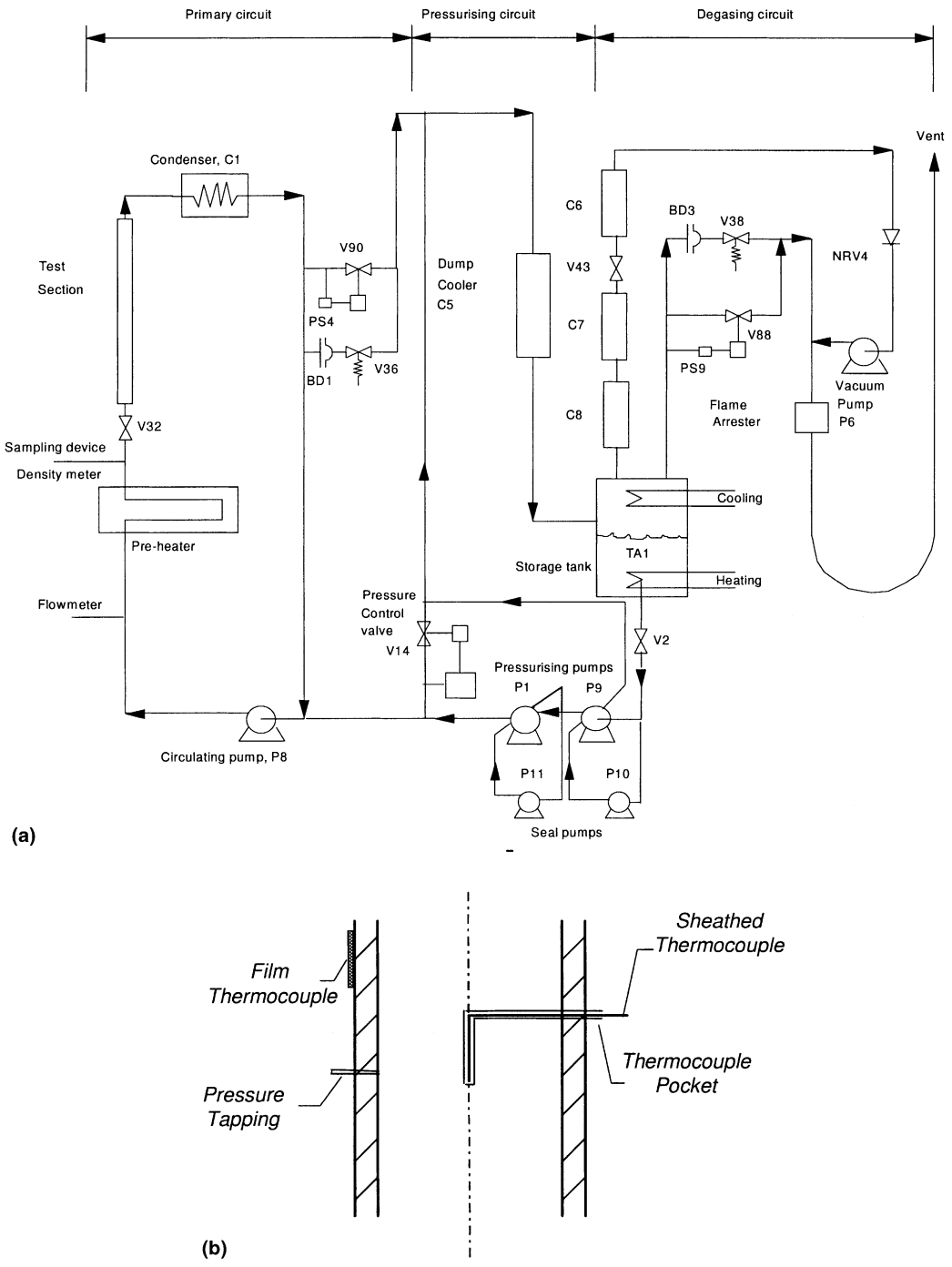


Fig. 1. (a) A schematic of the HTFS boiling facility; (b) drawing of the bulk thermocouple pocket.

Paar DPR 4/22 XEI) and a flowmeter (a drag disc device, model Ramapo Mark V-3/4-F02). The pressure is generated by two centrifugal pressurising pumps, pumping against a partly open control valve in the main loop. Fine adjustment of pressure is possible by speed control of the pressurising pumps. The test section is a 8.5 m long, 321 stainless steel tube with a nominal inner diameter of 25.4 mm and an outer diameter of 38.0 mm. Uniform heating can be achieved by Joule effect, passing a large DC current (up to 4000 A) at a low voltage (up to

30 V) through the test section wall. The non-uniformity of the heat generation due to changes in the electrical resistivity can be neglected since the changes in the wall temperature along the test section for boiling experiments are small. The test section is equipped with 70 thermocouples attached to the outer wall at a spacing of 100–150 mm. The inner wall temperature is calculated from the one-dimensional steady-state conduction equation, correcting for heat losses. The bulk temperature is measured at 12 locations along the test section (spaced at 750 mm intervals). To achieve the bulk temperature measurement, thermocouple pockets were created out of 2 mm diameter hypodermic tubes which were bent at a right angle and positioned at the centre line of the tube with the tip facing the flow (see Fig. 1(b)). The tips were sealed before the tubes were welded into position. In these pockets, sheathed thermocouples could be fed right into the tip. Three absolute pressure transducers (model Druck PDCR60) were located at the bottom, middle and top of the test section, with eight differential pressure cells (model Druck PDCR 120/75/WL/IS) located every 750 mm along the test section.

The bulk and wall thermocouples were checked against a calibrated dry block calibrator which had an accuracy of ±0.3 K. It was found that the thermocouple outputs were within the accuracy of the calibrator. Estimated uncertainties of measured values are presented in Table 1.

### 2.2. Experimental procedure and conditions

The boiling experiments were started at low heat flux, generally 10 kW $m^{-2}$ with the inlet temperature close to saturation, making sure that no vapour was generated in the preheater. This could be checked through the reading of a density meter placed immediately downstream of the preheater. In the main series of experiments, the heat flux was increased further in steps of 10 kW $m^{-2}$; to avoid dryout, the inlet temperature had often to be reduced with increasing heat flux. Another series of experiments were carried out where the heat flux, mass flux and pressure were kept constant and only the inlet temperature was increased up to a maximum value, typically 5–15 °C below saturation. In addition, runs with reduction in the inlet temperature were performed to allow examination of hysteresis effects. In this context, experiments were also conducted by increasing and decreasing the heat flux. A test matrix for the ternary mixture experiments is shown in Table 2.

Table 1
Uncertainty of measured values used in the determination of the experimental heat transfer coefficient

| | |
|---|---|
| Temperature (wall and bulk) | ±0.3 K |
| Pressure | 0.1% full scale |
| Voltage across the test section | ±1.0% |
| Current across the test section | ±1.0% |
| Thermal conductivity of the test section | ±4.0% |
| Heat loss | ±20% |
| Heated length | ±10 mm |
| Inner diameter of test section | ±0.1 mm |
| Test section wall thickness | ±0.15 mm |

Table 2
Test matrix for two-phase experiments

| Conditions | Unit | Range |
|---|---|---|
| Pressure | bar | 2.3, 3.0, 6.0, 10.0 |
| Mass flux | kg $m^{-2}$ $s^{-1}$ | 100, 200, 300, 500 |
| Heat flux | kW $m^{-2}$ | 10, 20, 30, 40, 50, 60, 70 |
| Inlet subcooling | K | Minimum of 5–15 |
| Exit quality | Dimensionless | $\leqslant 0.8$ |

## 3. Methodology

### 3.1. Interphase heat and mass transfer

The heat transfer coefficient in mixture systems is normally defined by the following equation:

$$\alpha = \frac{\dot{q}_w}{(T_w - T_E)}, \tag{1}$$

where $\dot{q}_w$ is the heat flux imposed to the walls of the tube, $T_w$ is the temperature of the inner wall of the tube and $T_E$ is the bubble point temperature (for boiling/evaporation) or the dew point temperature (for condensation). It is commonly acknowledged that heat transfer cofficients for mixtures are lower than those for pure fluids with identical physical properties. In the heat flux controlled case, such a deterioration in $\alpha$ is due to an increase in the wall temperature, $T_w$, and interface temperature, $T_I$, associated with mixture effects. As outlined by Wadekar [11], in the convective region where nucleate boiling is greatly suppressed, it can be postulated based on the calculations by Shock [12] that the *liquid film* heat transfer coefficient, $\alpha_{LF}$ is mainly a function of local turbulence and physical properties. Thus, to a first approximation, $(T_w - T_I)$ is given for a given heat flux and local quality. The heat transfer coefficient, $\alpha$, from the wall to the two-phase fluid mixture is usually defined from Eq. (1), with $T_E$ being determined from a flash calculation. If $T_I$ is higher than $T_E$, then $T_w$ is also higher and the value of $\alpha$ defined as $\dot{q}_w/(T_w - T_E)$ will be smaller. Two possible causes of an elevation of $T_I$ with respect to $T_E$ can be identified:

1. A difference could occur between the concentration of the components in the liquid film and their average

concentration in the entrained droplets. As discussed by Barbosa and Hewitt [1,2], the liquid film would have a higher concentration of the less volatile components than the droplets. Assuming, say, that the liquid film is fully internally mixed, then the equilibrium temperature at its interface would be higher than $T_E$, even in the absence of mass transfer resistances in the vapour.

2. The concentrations of the components at the interface are different from those in the bulk vapour. In order for the vapour generated at the interface to be transferred to the bulk vapour, concentration differences must also exist between the interface and the bulk vapour. This implies an elevation of the partial pressure at the interface and, consequently, an elevation of the interface temperature $T_I$ with respect to $T_E$.

Fig. 2 illustrates the geometry of the problem. The liquid phase is present as a climbing film coating the inner wall of the pipe and in the form of small droplets entrained in a vapour core. Droplet interchange between the core and the liquid film is modelled in terms of droplet entrainment and deposition rates [13].

Entrainment and deposition rates are calculated locally in terms of the local vapour velocity, the local film flow rate and the local droplet flow rate. The relationships used do not include any effect of heat flux on entrainment or deposition rate; such effects are discussed in detail by Barbosa et al. [14] who found that, based on established relationships for the effect of heat flux on entrainment, the effect was negligible in the conditions of the current experiment.

The gas phase is a saturated or subcooled mixture which may contain non-condensing gases as well as vapours. All the resistances to heat and mass transfer in the gas side are assumed to lie in thin layers of thicknesses $s_h$ and $s_m$ adjacent to the interface. The flow in such layers is assumed to be steady, laminar, and one-dimensional. Transport properties are considered constant. Homogeneous chemical reactions, viscous dissipation, and radiant-emission or absorption in the fluid are neglected.

The total rate of energy transport to the vapour in the core is given by a sum of latent and sensible heat contributions,

$$\dot{q}_{GC} = \sum_{j=1}^{3} \dot{m}_{I,j} \Delta h_{v,j} + \alpha'_{GC} e^{\phi_T} (T_I - T_C), \tag{2}$$

where

$$\alpha'_{GC} = \frac{\alpha_{GC} \phi_T}{e^{\phi_T} - 1}, \tag{3}$$

and

$$\phi_T = \frac{1}{\alpha_{GC}} \sum_{j=1}^{3} \dot{m}_{I,j} c_{pGC,j}. \tag{4}$$

The heat transfer coefficient is calculated using a Dittus–Boelter type relationship

$$\frac{\alpha_{GC} d_T}{\lambda_{GC}} = 0.023 Re_{GC}^{0.8} Pr_{GC}^{0.4}. \tag{5}$$

Interfacial mass transfer plays a significant role in the evaporation process. The combined effect of differences

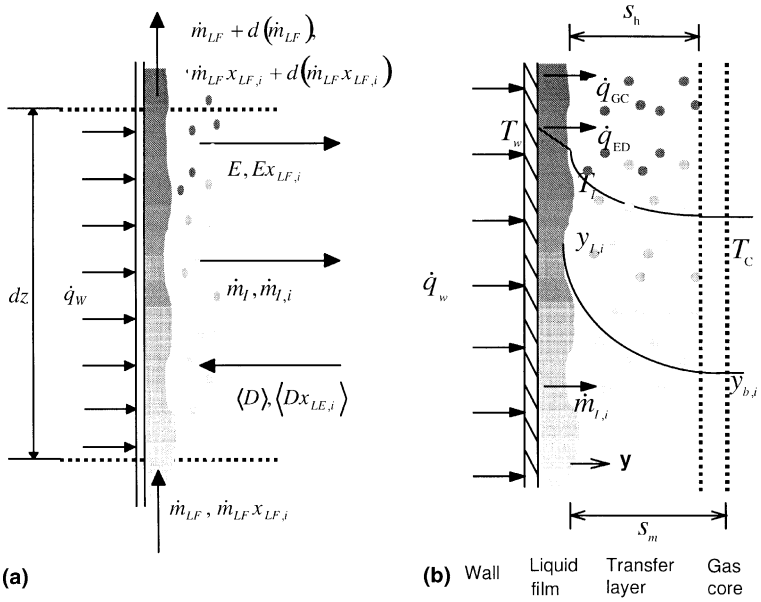


Fig. 2. The model geometry. (a) Hydrodynamics; (b) heat and mass transfer.

in concentration between the droplets and the film and of vapour phase mass transfer was discussed for the binary case in [1,2]. For the ternary case, the situation is somewhat more complicated. One may either use an *effective diffusivity* for each of the components. This approach ignores *interactions* between the respective fluxes and the more comprehensive approach is to take account of these interactions. Both approaches were pursued in this work.

Fick's Law for the layer geometry is given by

$$\dot{m}_{\mathrm{I},i} = y_{\mathrm{I},i}\sum_{j=1}^{3}\dot{m}_{\mathrm{I},j} - \rho_{\mathrm{GC}}\sum_{k=1}^{2}\Delta_{i,k}\frac{\mathrm{d}y_k}{\mathrm{d}y}. \tag{6}$$

In terms of the elements of a finite-flux matrix of mass transfer coefficients, the evaporating mass flux vector is as follows [8]:

$$\dot{m}_{\mathrm{I},i} = y_{\mathrm{I},i}\sum_{j=1}^{3}\dot{m}_{\mathrm{I},j} + \rho_{\mathrm{GC}}\sum_{k=1}^{2}B^{\cdot}_{\mathrm{G}_{i,k}}(y_{\mathrm{I},i} - y_{\mathrm{b},i}), \tag{7}$$

where

$$[B^{\cdot}_{\mathrm{G}}] = [B_{\mathrm{G}}][\Phi]\{\exp[\Phi] - [I]\}^{-1}, \tag{8}$$

and

$$[\Phi] = \frac{1}{\rho_{\mathrm{GC}}}\sum_{j=1}^{3}\dot{m}_{\mathrm{I},j}[B_{\mathrm{G}}]^{-1}. \tag{9}$$

The zero-flux matrix of mass transfer coefficients is also given by a Dittus–Boelter type relationship. As suggested by Webb et al. [15], no enhancement due to interfacial wave effects or entrainment was taken into account in such calculations.

$$[B_{\mathrm{G}}]d_{\mathrm{T}}[\Delta]^{-1} = 0.023Re_{\mathrm{GC}}^{0.8}[Sc_{\mathrm{GC}}]^{0.4}, \tag{10}$$

where

$$[Sc_{\mathrm{GC}}] = \frac{\rho_{\mathrm{GC}}}{\eta_{\mathrm{GC}}}[\Delta]^{-1}, \tag{11}$$

and $[\Delta]$ is the matrix of Fickian diffusion coefficients.

The diffusivity fluxes are given by the second term on the RHS of Eqs. (6) and (7). Unlike the binary case, for multicomponent systems the concentration gradients of each component may be different. If the elements off the main diagonal of $[\Delta]$ are not equal to zero, then interaction effects [16] are bound to occur.

Taylor and Krishna [8] pointed out a criterion for quantifying diffusive interaction effects. This is as follows (in terms of a matrix of mass transfer coefficients),

$$I_{\mathrm{p}_i} = \frac{|\,B^{\cdot}_{\mathrm{G}_{ij}}(y_{\mathrm{I},j} - y_{\mathrm{b},j})\,|}{|\,B^{\cdot}_{\mathrm{G}_{ii}}(y_{\mathrm{I},i} - y_{\mathrm{b},i})\,|} \sim \mathrm{O}(1). \tag{12}$$

Thus, the higher $I_{\mathrm{p}_i}$, the higher the significance of interaction effects, e.g., the tendency of species $i$ to diffuse in a direction opposite to that indicated by its own gradient of concentration (*reverse diffusion*).

The matrix of Fickian diffusion coefficients is calculated depending on the formulation (interactive or effective diffusivity) chosen. These are summarised below.

### 3.1.1. Interactive method

In the interactive approach, the elements of $[\Delta]$ for a ternary system are given by [8],

$$\Delta_{11} = \delta_{13}[y_{\mathrm{b},1}\delta_{23} + (1 - y_{\mathrm{b},1})\delta_{12}]/S, \tag{13}$$

$$\Delta_{12} = y_{\mathrm{b},1}\delta_{23}(\delta_{13} - \delta_{12})/S, \tag{14}$$

$$\Delta_{21} = y_{\mathrm{b},2}\delta_{13}(\delta_{23} - \delta_{12})/S, \tag{15}$$

$$\Delta_{22} = \delta_{23}[y_{\mathrm{b},2}\delta_{13} + (1 - y_{\mathrm{b},2})\delta_{12}]/S, \tag{16}$$

where $S = y_{\mathrm{b},1}\delta_{23} + y_{\mathrm{b},2}\delta_{13} + y_{\mathrm{b},3}\delta_{12}$.

### 3.1.2. Effective diffusivity method

In this approach, only the main diagonal elements of the matrix of Fickian diffusion coefficients are different than zero. These are given by

$$\Delta_{ii} = \delta_{i3}, \tag{17}$$

where $i = 1, 2$.

Therefore, interaction effects are not accounted for by the Effective Diffusivity Method.

It is also assumed that there is no direct interaction between entrainment, deposition and the diffusive processes (though the concentrations involved will be affected by entrainment and deposition in the manner described above).

In both formulations, the coefficients were obtained assuming ideal gas behaviour in the vapour side. The Maxwell–Stefan diffusion coefficients, $\delta_{ij}$, for the binary pairs are calculated through the correlation of Fuller et al. [17].

Eq. (7) is not a complete description of the evaporation process as only its diffusional part was specified. Another relationship is needed (determinacy condition) so that the overall interfacial flux is known. For the present geometry and flow regime in the liquid film, the *fully mixed liquid* determinacy condition, seems more appropriate (the action of disturbance waves is towards a homogenisation of the concentration in the film). In this case, the interfacial liquid composition is known a priori (previous liquid film evaporation and a bubble point calculation defines the interfacial state (vapour composition and inter facial temperature) of the vapour.

An additional closure hypothesis is as follows:

$$\dot{q}_{\mathrm{GC}} = \dot{q}_{\mathrm{w}} - \dot{q}_{\mathrm{ED}}, \tag{18}$$

where

$$\dot{q}_{\mathrm{ED}} = (E - \langle D\rangle)c_{\mathrm{pLE}}(T_{\mathrm{I}} - T_{\mathrm{C}}), \tag{19}$$

is the energy released/absorbed by the entrained droplets due to entrainment and deposition. The operator $\langle\ \rangle$ defines the cumulative value of a given parameter at a given distance. For instance, $\langle D^m\rangle = \sum_{j=0}^{m} D^{j,m}$ is the deposition rate of droplets entrained at a section $j$ (upstream to $m$) that deposit at a section $m$. The calculation of cumulative parameters is, as will be seen, of particular importance due to the axial gradient of concentration in the liquid film as the more volatile component preferentially evaporates.

### 3.2. Conservation equations and closure

Momentum, mass and energy conservation equations are solved for the annular flow regime. Detailed information about the derivation and solution of the set of conservation equations are given by Barbosa and Hewitt [1,2]. Here, it suffices to say that the difference in volatility between the components gives rise to axial gradients of concentration in both liquid and vapour streams due to the preferential evaporation of the more volatile component(s) even when local component equilibrium occurs. In annular flow, such an equilibrium situation is broken down by droplet entrainment and deposition since liquid is exchanged between different sections of the pipe. Moreover, the droplets themselves, at a given distance, will have a mean concentration different from that of the liquid film. A simplified approach to the phenomenon pursued here suggests that, if the vaporisation rate of the liquid film is much higher than that of the droplets in the core, then it is not illogical to assume that, whilst in the vapour core, the droplets retain a, concentration approximately equal to that of the liquid film at the point where they were created (entrained). Thus, droplets generated at distinct co-ordinates have distinct concentrations and, at a particular co-ordinate, a spectrum of concentration is found in the population of depositing droplets.

The conservation equations for the ternary mixture case are as follows:

$$\frac{\mathrm{d}}{\mathrm{d}z}\dot{m}_{\mathrm{LF}} = \frac{4}{d_{\mathrm{T}}}\left(\langle D\rangle - E - \sum_{j=1}^{3}\dot{m}_{\mathrm{I},j}\right), \tag{20}$$

$$\frac{\mathrm{d}}{\mathrm{d}z}\dot{m}_{\mathrm{GC}} = \frac{4}{d_{\mathrm{T}}}\sum_{j=1}^{3}\dot{m}_{\mathrm{I},j}, \tag{21}$$

$$\frac{\mathrm{d}}{\mathrm{d}z}\dot{m}_{\mathrm{LE}} = \frac{4}{d_{\mathrm{T}}}(E - \langle D\rangle), \tag{22}$$

$$\frac{\mathrm{d}}{\mathrm{d}z}x_{\mathrm{LF},i} = \frac{4}{d_{\mathrm{T}}\dot{m}_{\mathrm{LF}}}\left[(\langle Dx_{\mathrm{LF},i}\rangle - \langle D\rangle x_{\mathrm{LF},i}) + \sum_{j=1}^{3}\dot{m}_{\mathrm{I},j}x_{\mathrm{LF},i} - \dot{m}_{\mathrm{I},i}\right], \tag{23}$$

$$\dot{m}_{\mathrm{C}}c_{\mathrm{pC}}\frac{\mathrm{d}}{\mathrm{d}z}T_{\mathrm{C}} = \frac{4}{d_{\mathrm{T}}}[\alpha^{\bullet}_{\mathrm{GC}}(T_{\mathrm{I}} - T_{\mathrm{C}}) + (E - \langle D\rangle)c_{\mathrm{pLE}}(T_{\mathrm{I}} - T_{\mathrm{C}})]. \tag{24}$$

Eqs. (20)–(22) represent overall mass conservation for the liquid film, vapour core and liquid entrained as droplets. Eq. (23) is a component mass balance for the liquid film. The effect of deposition of droplets having different concentrations is characterised by the expression in parenthesis in the RHS of (23). Eq. (24) is an energy balance for the core, the first term in the RHS of (24) is the conductive contribution of the heat flux to the vapour phase. The second term is the net energy released/absorbed by the entrained liquid due to entrainment and deposition, $\dot{m}_{\mathrm{C}}, c_{\mathrm{pC}}$ and $T_{\mathrm{C}}$ are the homogeneous core mass flux, specific heat capacity and temperature, respectively. These are given by

$$\dot{m}_{\mathrm{C}} = \dot{m}_{\mathrm{GC}} + \langle\dot{m}_{\mathrm{LE}}\rangle, \tag{25}$$

$$c_{\mathrm{pC}} = \frac{\dot{m}_{\mathrm{GC}} + \langle\dot{m}_{\mathrm{LE}}\rangle}{\frac{\dot{m}_{\mathrm{GC}}}{c_{\mathrm{pGC}}} + \left\langle\frac{\dot{m}_{\mathrm{LE}}}{c_{\mathrm{pLE}}}\right\rangle}, \tag{26}$$

and

$$T_{\mathrm{C}} = \frac{\dot{m}_{\mathrm{GC}}c_{\mathrm{pGC}} + \langle\dot{m}_{\mathrm{LE}}c_{\mathrm{pLE}}\rangle}{\frac{\dot{m}_{\mathrm{GC}}c_{\mathrm{pGC}}}{T_{\mathrm{GC}}} + \left\langle\frac{\dot{m}_{\mathrm{LE}}c_{\mathrm{pLE}}}{T_{\mathrm{LE}}}\right\rangle}. \tag{27}$$

A conservation equations for the bulk vapour concentration is given by

$$\frac{\mathrm{d}}{\mathrm{d}z}y_{\mathrm{b},i} = \frac{4}{d_{\mathrm{T}}\dot{m}_{\mathrm{GC}}}\left(\dot{m}_{\mathrm{I},i} - \sum_{j=1}^{3}\dot{m}_{\mathrm{I},j}y_{\mathrm{b},i}\right). \tag{28}$$

Momentum balance equations for the annular flow regime were solved together with the mass balance relationships described above. These will not be repeated here and can be found elsewhere [1,2,18].

At each integration step $\Delta z$, an iterative procedure is carried out to determine the interfacial mass fluxes, compositions and temperature. The solution algorithm for the interphase heat and mass transfer calculation is comprised of the following steps [6]:

1. *Known*: $x_{\mathrm{LF}_{\mathrm{I},i}}(= x_{\mathrm{LF}_{\mathrm{b},i}}$, fully mixed film hypothesis), $y_{\mathrm{b},i}, T_{\mathrm{C}}$.
2. *Calculate*: $y_{\mathrm{I},i}, T_{\mathrm{I}} \rightarrow$ Bubble point temperature subroutine.
3. *Guess*: $\sum_{j=1}^{3}\dot{m}_{\mathrm{I},j}$.
4. *Calculate*: $\frac{\dot{m}_{\mathrm{I},j}}{\sum_{j=1}^{3}\dot{m}_{\mathrm{I},j}} \rightarrow$ Eq. (7).
5. *Calculate*: $\dot{q}_{\mathrm{GC}} \rightarrow$ Eq. (2)
6. *Compare*: If $\dot{q}_{\mathrm{GC}} \neq \dot{q}_{\mathrm{w}} - \dot{q}_{\mathrm{ED}}$, update $\sum_{j=1}^{3}\dot{m}_{\mathrm{I},j}$ and return to step 4.

Finally, $T_{\mathrm{w}}$ is calculated as follows:

$$T_{\mathrm{w}} = T_{\mathrm{I}} + \frac{\dot{q}_{\mathrm{w}}}{\alpha_{\mathrm{LF}}}, \tag{29}$$

where $\alpha_{LF}$ is the heat transfer coefficient for the liquid film calculated using the correlation of Chen [19] with the (small) nucleate boiling component corrected for mixture effects as suggested by Palen and Small [20].

As pointed out in previous work [1,2], a significant amount of liquid may be entrained as droplets at the onset of annular flow, perhaps as a result of high liquid entrainment also present in the churn flow regime [21]. There is at present no general method for calculating the entrained fraction at the onset of annular flow. Thus, the approach of assuming a series of values covering the likely range (i.e., 0%, 10%, 20% and 40%) and carrying out calculations for each of these values is undertaken here.

Thermodynamic and transport properties were calculated using the various methods described by Assael et al. [22].

## 4. Results

Figs. 3 and 4 illustrate typical variations of liquid phase (film and droplets) mean concentration and of bulk and interfacial vapour concentrations calculated using an Interactive formulation. As will be seen in Fig. 5, which shows a plot of the interaction parameters $I_{p1}$ and $I_{p2}$, interaction effects are not important for the cases studied. For other runs, the values of $I_{pi}$ were never higher than $10^{-3}$. Therefore, for the conditions evaluated, diffusive interaction effects are not relevant.

Figs. 6(a) and (b) show the predictions of wall, interface and core temperatures for different initial entrained fractions at various conditions. A variation in the initial entrained fraction provokes an opposite effect in the behaviour of mean temperatures; higher values of initial $\dot{m}_{LE}$ induce lower profiles of $T_C$ and higher profiles of $T_I$. As observed in the binary mixture temperature predictions [2], the measured temperature trends are well picked up by the formulation, but the agreement somewhat decreases with increasing pressure.

The measured heat transfer coefficients (calculated by introducing the known wall heat flux, the measured wall temperature and the calculated value of $T_E$ into Eq. (1))

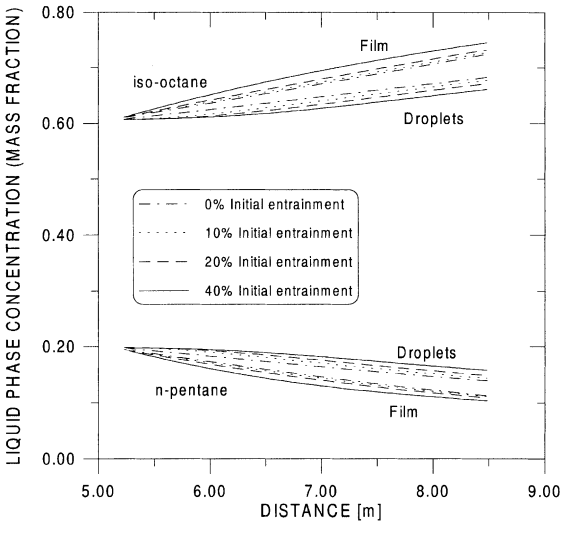


Fig. 3. Profiles of liquid phase concentration. $p = 2.3$ bar, $\dot{m}_T = 297.54$ kg m$^{-2}$ s$^{-1}$, $\dot{q}_w = 40.51$ kW m$^{-2}$.

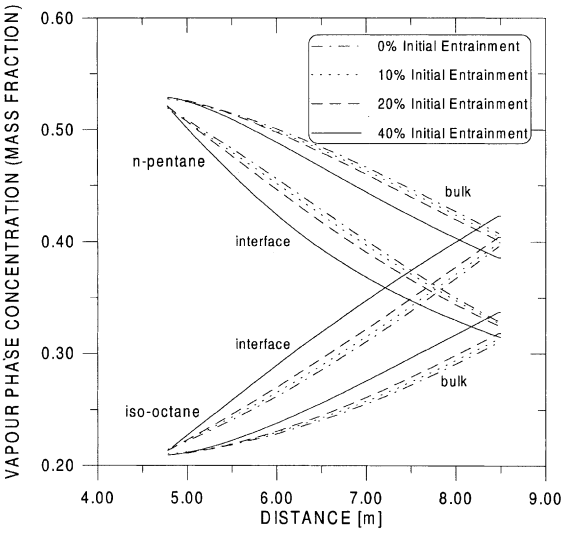


Fig. 4. Profiles of vapour phase concentration. Same conditions as in Fig. 3.

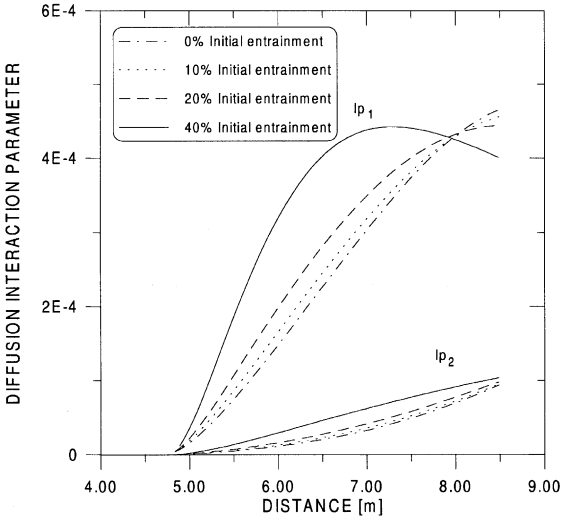


Fig. 5. A typical distribution of Diffusion Interaction Parameters. $p = 3.14$ bar, $\dot{m}_T = 295.98$ kg m$^{-2}$ s$^{-1}$, $\dot{q}_w = 49.50$ kW m$^{-2}$.

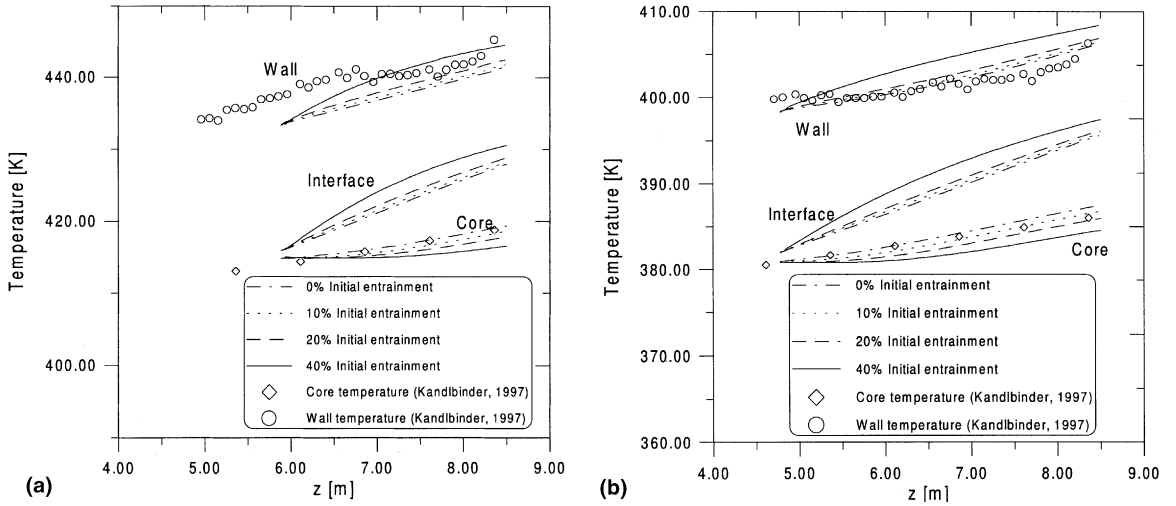


Fig. 6. Distributions of wall, interface and core temperatures: (a) $p = 6.03$ bar, $\dot{m}_T = 300.48$ kg m$^{-2}$ s$^{-1}$, $\dot{q}_w = 48.91$ kW m$^{-2}$; (b) $p = 3.14$ bar, $\dot{m}_T = 295.98$ kg m$^{-2}$, $\dot{q}_w = 49.50$ kW m$^{-2}$.

are compared with those calculated using the present methodology in Figs. 7(a) and (b). Again, the capability of the formulation at predicting the decrease in the heat transfer coefficient with increasing quality is well observed.

The predictions in Figs. 6 and 7 were obtained applying the Effective Diffusivity Method. As seen before, the difference between the results given by this method and those given by the Interactive Method is negligible. The computing time, however, is as expected, shorter for the Effective Diffusivity Method.

Fig. 8 shows a comparison between experimental and predicted heat transfer coefficients averaged over the segment of pipe over which annular flow took place. The average heat transfer coefficient is defined by

$$\alpha_{av} = \frac{1}{L_A}\int_0^{L_A} \alpha \, dz. \tag{30}$$

The agreement is good, with the majority of data points lying within the ±20% error boundary. It was found that the data points that presented the largest deviation (out-side that range) were those obtained at high pressure (10 bar), low total mass flowrate (100, 200 kg m$^{-2}$ s$^{-1}$) and high wall heat flux (50, 60 kW m$^{-2}$). This may be due to presence of additional nucleate boiling or due to an unsuitability of some methods and

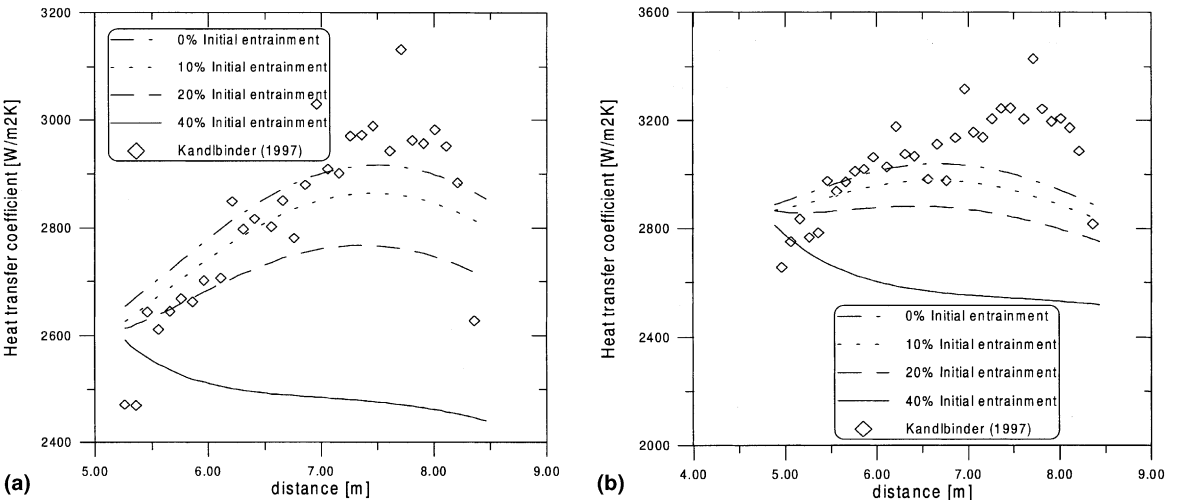


Fig. 7. Distributions of local heat transfer coefficient. (a) $p = 2.3$ bar, $\dot{m}_T = 297.54$ kg m$^{-2}$ s$^{-1}$, $\dot{q}_w = 40.51$ kW m$^{-2}$; (b) $p = 3.14$ bar, $\dot{m}_T = 295.98$ kg m$^{-2}$ s$^{-1}$, $\dot{q}_w = 49.50$ kW m$^{-2}$.

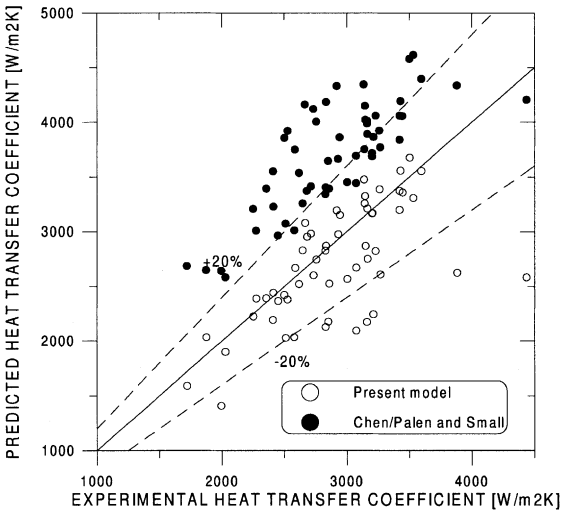


Fig. 8. Comparison of average heat transfer coefficients.

correlations employed in the model to deal with higher pressures. The predicted heat transfer coefficients were obtained using an initial entrained fraction of 10% for this being a value close to that estimated for hydrodynamic equilibrium (equal entrainment and deposition rates).

The predictions obtained with the Chen [19] correlation using the correction factor by Palen and Small [20] for mixture effects, but not taking account of droplet and interfacial mass transfer effects are also shown for comparison purposes. A considerable overprediction of the heat transfer coefficient is given by this method.

## 5. Conclusions

Forced convective boiling experiments were carried out in a vertical tube using a ternary *n*-pentane/*n*-hexane/iso-octanc mixture. A decrease in the local heat transfer coefficient was observed and an extension to ternary mixtures of a model for forced convective boiling of binary mixtures in annular flow [1,2] was proposed so as to predict such trends. Interphase transfer of mass and heat was dealt with using a Colburn method with the diffusive fluxes modelled via a linearly generalised Fick's Law [3,4] or via an Effective Diffusivity formulation.

Basically, the discrepancies with normal prediction methods arise for two reasons, mainly differences in concentration which develop between the droplets and the liquid film at given locations along the channel (whereas the normal methodologies implicitly assume that the concentrations are identical in the whole liquid phase) and, secondly, the complexities of interfacial mass transfer giving temperature differences between the interface and the vapour core. The methodology proposed here deals with both these effects. The droplet transport is dealt with by dealing locally with entrainment and deposition and by 'book-keeping' on the concentration of the three components in the droplets.

As for the binary case, the model predictions for temperature and heat transfer coefficient distributions are in quite good agreement. Diffusive interaction effects were found to be not important for the set of conditions assessed.

## Acknowledgements

The first author thanks the Brazilian National Research Council (CNPq – Conselho Nacional de Desenvolvimento Científico e Tecnológico) for the award of a scholarship (Grant No. 200085/97-2). The Heat Transfer and Fluid Flow Service (HTFS) of AEA Technology plc provided the laboratory facilities and the support services. The research funding was provided by the Engineering and Physical Sciences Research Council (EPSRC).

## References

[1] J.R. Barbosa Jr., G.F. Hewitt, Forced convective boiling of binary mixtures in annular flow. Part I: Liquid phase mass transport, Int. J. Heat Mass Transfer 44 (2001) 1465–1474.
[2] J.R. Barbosa Jr., G.F. Hewitt, Forced convective boiling of binary mixtures in annular flow. Part II: Heat and mass transfer, Int. J. Heat Mass Transfer 44 (2001) 1475–1484.
[3] H.L. Toor, Solution of the linearized equations of multicomponent mass transfer. Part II: matrix methods, AIChE J. 10 (4) (1964) 460–465.
[4] W.E. Stewart, R. Prober, Matrix calculation of multicomponent mass transfer in isothermal systems, Ind. Eng. Chem. Fundam. 3 (3) (1964) 224–235.
[5] T. Kandlbinder, Experimental investigation of forced convective boiling of hydrocarbons and hydrocarbon mixtures, Ph.D. Thesis, University of London, Imperial College, UK, 1997.
[6] D.R. Webb, Heat and mass transfer in condensation of multicomponent vapours, in: U. Grigull (Ed.), Proceedings of the Seventh Heat Transfer Conference, Hemisphere, New York, 1982, pp. 167–174.
[7] S. Koyama, S.M. Lee, A prediction model for condensation of ternary refrigerant mixtures inside a horizontal smooth tube, in: J.S. Lee (Ed.), Proceedings of the Eleventh Heat Transfer Conference, Taylor & Francis, Philadelphia, PA, 1998, pp. 427–432.
[8] R. Taylor, R. Krishna, Multicomponent Mass Transfer, Wiley, New York, 1993.
[9] D.R. Webb, Condensation of vapour mixtures, in: G.F. Hewitt (Ed.), Handbook of Heat Exchanger Design, second ed., Begell House Incorporation, New York, 1995, pp. 2.6.3-1–2.6.3-25.

[10] L. Zhang, E. Hihara, T. Saito, J.T. Oh, Boiling heat transfer of a ternary refrigerant mixture inside a horizontal smooth tube, Int. J. Heat Mass Transfer 40 (9) (1997) 2009–2017.
[11] V.V. Wadekar, Convective heat transfer to binary mixtures in annular two-phase flow, in: G.F. Hewitt (Ed.), Proceedings of the 10th Heat Transfer Conference, Taylor & Francis, Philadelphia, PA, 1994, pp. 557–562.
[12] R.A.W. Shock, Evaporation of binary mixtures in upward annular flow, Int. J. Multiphase Flow 2 (1976) 411–433.
[13] A.H. Govan, G.F. Hewitt, D.G. Owen, T.R. Bott, An improved CHF modelling code, in: Proceedings of the Second UK National Heat Transfer Conference, Institution of Mechanical Engineers, London, UK, 1988, pp. 33–48.
[14] J.R. Barbosa Jr., T. Kandlbinder, G.F. Hewitt, A study of dryout in annular flow of single component hydrocarbons and their mixtures, Multiphase Sci. Technol. 12 (3/4) (2000) 265–293.
[15] D.R. Webb, M. Fahrner, R. Schwaab, The relationship between the Colburn and Silver methods for condenser design, Int. J. Heat Mass Transfer 39 (15) (1993) 3147–3156.
[16] H.L. Toor, Diffusion in three component gas mixtures, AIChE J. 3 (1957) 198–207.
[17] E. Fuller, P.D. Schettler, J.C. Giddings, A new method for prediction of binary gas phase diffusion coefficients, Ind. Eng. Chem. 58 (5) (1966) 19–23.
[18] N.J. Hawkes, Wispy-annular flow, Ph.D. Thesis, University of London, Imperial College, UK, 1996.
[19] J.C. Chen, A correlation for boiling heat transfer to saturated fluids in convective flow, ASME-AIChE Heat Transfer Conference, Boston, MA, 1963, Paper 63-HT-34.
[20] J.W. Palen, W.M. Small, A new way to design kettle and internal reboilers, Hydrocarbon Process. 43 (11) (1964) 199–208.
[21] G.F. Hewitt, N.S. Hall-Taylor, Annular Two-Phase Flow, Pergamon Press, London, 1970.
[22] M.J. Assael, J.P.M. Trusler, T.F. Tsolakis, Thermophysical Properties of Fluids, Imperial College Press, London, 1996.